

Hot Spot Offset Variability from Magnetohydrodynamical Thermoresistive Instability (TRI) in Hot Jupiters

Raphaël Hardy^{1,2,3}, Paul Charbonneau¹, Andrew Cumming^{2,3}

¹Département de Physique, Université de Montréal, Montréal, QC, H3C 3J7, Canada

²Department of Physics and Trottier Space Institute, McGill University, Montréal, QC, H3A 2T8, Canada

³Institut Trottier de Recherche sur les Exoplanètes (iREx), Université de Montréal, Montréal, QC H3C 3J7, Canada

The first work in this series presents a local model of the TRI.



The second work in this series presents a 1D radial model of the TRI.



1. BACKGROUND

Hot Jupiters' atmospheric dynamics are shaped by intense radiation from their host stars and tidal locking, causing large temperature gradients and equatorial superrotating jets. These jets are usually prograde, but some exhibit retrograde motion (e.g. Bell et al. 2021). Magnetic effects, coming from partial ionization of alkali metals, can lead to retrograde winds and westward hot spots. Studies have shown magnetic coupling between upper atmosphere winds and planetary interior magnetic fields (e.g. Rogers & Komacek 2014). The ionization fraction's sensitivity to temperature changes affects magnetic coupling, and leads to a **thermoresistive instability (TRI)**, where ohmic heating leads to atmospheric runaway heating (Menou 2012, Hardy et al. 2022, 2023).

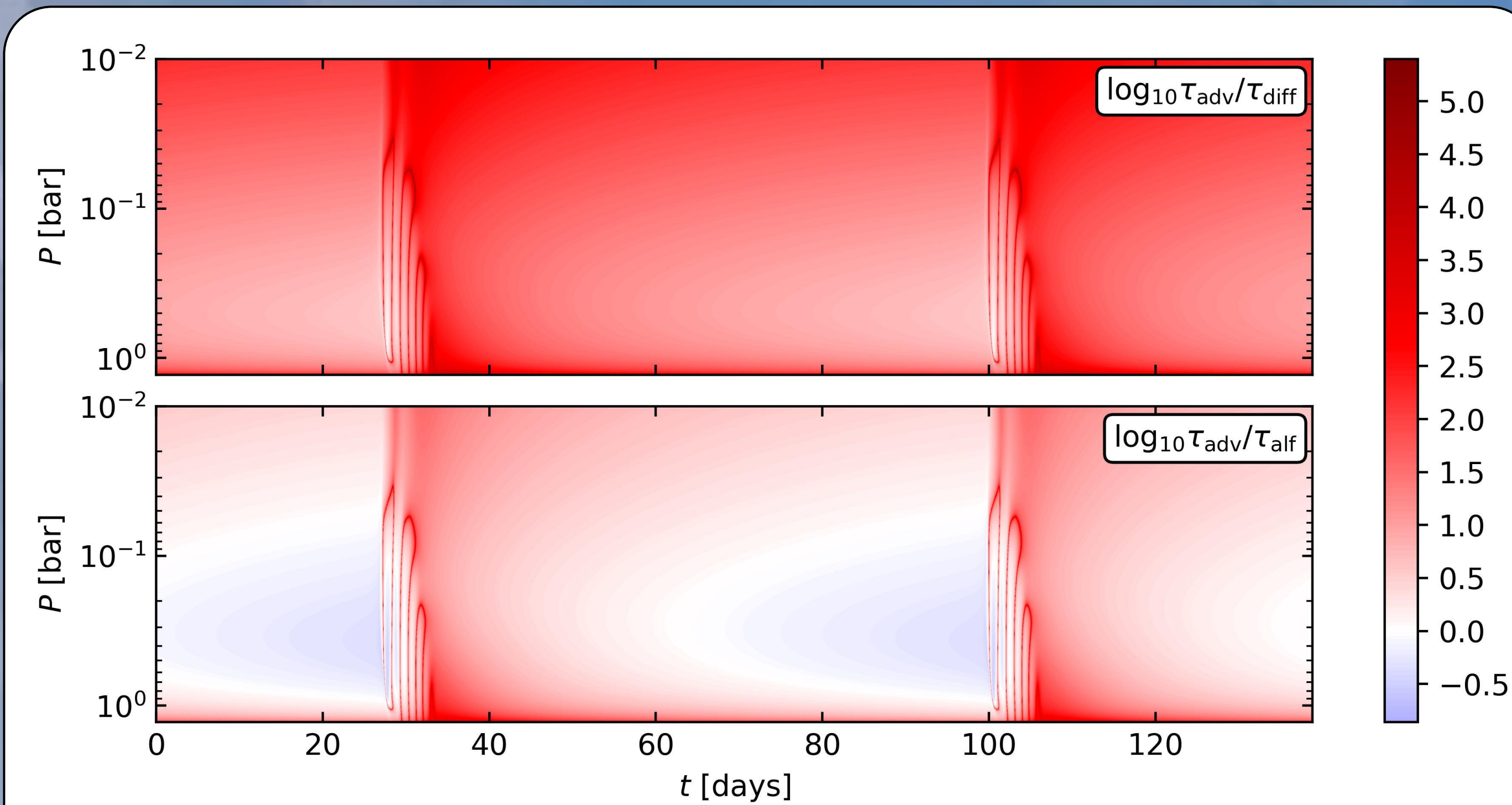


Figure 1 : Ratios of timescales at play in the system during oscillations. The length scale used is the pressure scale height for τ_{alf} and τ_{diff} which we update with temperature at the substellar point at every time step and the radius is used for τ_{adv} .

2. MODEL

We present a 1D radial model of a thin Hot Jupiter's atmosphere in the equatorial plane. Using first-order Fourier expansions, we expand temperature and magnetic diffusivity in the longitudinal direction. Assuming a non-compressible fluid and Gauss' law for magnetism, the velocity and magnetic field must be axisymmetric. Hence, our equations are :

$$\begin{aligned} \mathbf{B}(z) &= B_x(z)\hat{x} + B_0\hat{z} \\ \tilde{T}(\phi) &= T_0 + T_1 \sin \phi + T_2 \cos \phi \\ \tilde{\eta}(\phi) &= \eta_0 + \eta_1 \sin \phi + \eta_2 \cos \phi \\ \eta(\phi) &= 0.023 \frac{\tilde{T}^{1/2}(\phi)}{\chi_e} \text{ m}^2 \text{ s}^{-1} \\ \eta_0 &= \sum_{\phi} \frac{\eta(\phi)}{n} \\ \eta_1 &= \frac{\sum_{\phi} \eta(\phi) \sin \phi}{\sum_{\phi} \sin^2 \phi} \\ \eta_2 &= \frac{\sum_{\phi} \eta(\phi) \cos \phi}{\sum_{\phi} \cos^2 \phi} \end{aligned}$$

$$\begin{aligned} \frac{\partial T_0}{\partial t} &= \frac{1}{\rho c_p} \frac{\partial \bar{\chi}}{\partial z} \frac{\partial T_0}{\partial z} + \frac{\bar{\chi}}{\rho c_p} \frac{\partial^2 T_0}{\partial z^2} + \frac{1}{2} \frac{1}{\rho c_p} \frac{\partial F_{\text{irr}}}{\partial z} + \frac{\bar{\mu}}{\rho c_p} \left(\frac{\partial u_x}{\partial z} \right)^2 + \frac{\eta_0}{\mu_0 \rho c_p} \left(\frac{\partial B_x}{\partial z} \right)^2 \\ \frac{\partial T_1}{\partial t} &= \frac{u_x T_2}{R} + \frac{1}{\rho c_p} \frac{\partial \bar{\chi}}{\partial z} \frac{\partial T_1}{\partial z} + \frac{\bar{\chi}}{\rho c_p} \frac{\partial^2 T_1}{\partial z^2} + \frac{1}{2} \frac{1}{\rho c_p} \frac{\partial F_{\text{irr}}}{\partial z} + \frac{\eta_1}{\mu_0 \rho c_p} \left(\frac{\partial B_x}{\partial z} \right)^2 \\ \frac{\partial T_2}{\partial t} &= -\frac{u_x T_1}{R} + \frac{1}{\rho c_p} \frac{\partial \bar{\chi}}{\partial z} \frac{\partial T_2}{\partial z} + \frac{\bar{\chi}}{\rho c_p} \frac{\partial^2 T_2}{\partial z^2} + \frac{\eta_2}{\mu_0 \rho c_p} \left(\frac{\partial B_x}{\partial z} \right)^2 \\ \frac{\partial B_x}{\partial t} &= B_0 \frac{\partial u_x}{\partial z} + \frac{\partial \eta_0}{\partial z} \frac{\partial B_x}{\partial z} + \eta_0 \frac{\partial^2 B_x}{\partial z^2} \\ \frac{\partial u_x}{\partial t} &= \frac{B_0}{\mu_0 \bar{\rho}} \frac{\partial B_x}{\partial z} + \frac{\bar{\mu}}{\bar{\rho}} \frac{\partial^2 u_x}{\partial z^2} + a_x \end{aligned}$$

3. RESULTS

- Thermal diffusion dominates, limiting the hot spot's longitudinal range. The interplay of advection and Alfvénic timescales causes interesting **non-linear motions during oscillations**.
- Alfvénic oscillations and temperature runaway occur at depth in the atmosphere.
- The hottest point can extend beyond the terminators but does so when the atmospheric temperature is almost uniform in longitude.
- Figure 2 shows the key to TRI ; $Rm < 1$ before and after the instability and $Rm > 1$ during.**
- The thermal runaway from TRI alters thermal flux at the upper boundary, artificially amplified by the constant temperature boundary condition.
- TRI and following Alfvénic oscillations lead to **significant longitudinal variations in hot spot position, which could be observed.**

4. TAKE-AWAYS

- The model helps characterize hot spot offsets in response to atmospheric forcing and TRI. **Simulations suggest TRI's potential observability in Hot Jupiter atmospheres, causing significant offset variations** within reasonable bounds compared to observations (Bell et al. 2021).
- Comparisons with Keating et al. (2019) indicate the model may underestimate temperature contrasts between day and night sides. Thermal runaway leads to notable flux variation, **potentially indicating TRI occurrence in unexpectedly bright planets**. However, model limitations, such as fixed temperature at the upper boundary and assumptions of axisymmetric dynamics, could inflate flux deviations.
- Simulations demonstrate that **magnetic field strength influence recurrence periods and oscillation amplitudes**. Magnetic field strengths suggested by Yadav et al. (2017) may support TRI under appropriate conditions.
- Incorporating temperature-dependent magnetic diffusivity in atmospheric models significantly impacts dynamics, especially when the **magnetic Reynolds number nears unity in Hot Jupiters with low to moderate equilibrium temperatures**. Future models should include these dependencies and all relevant physical mechanisms for better predictions of TRI-induced offset variability and luminosity changes.

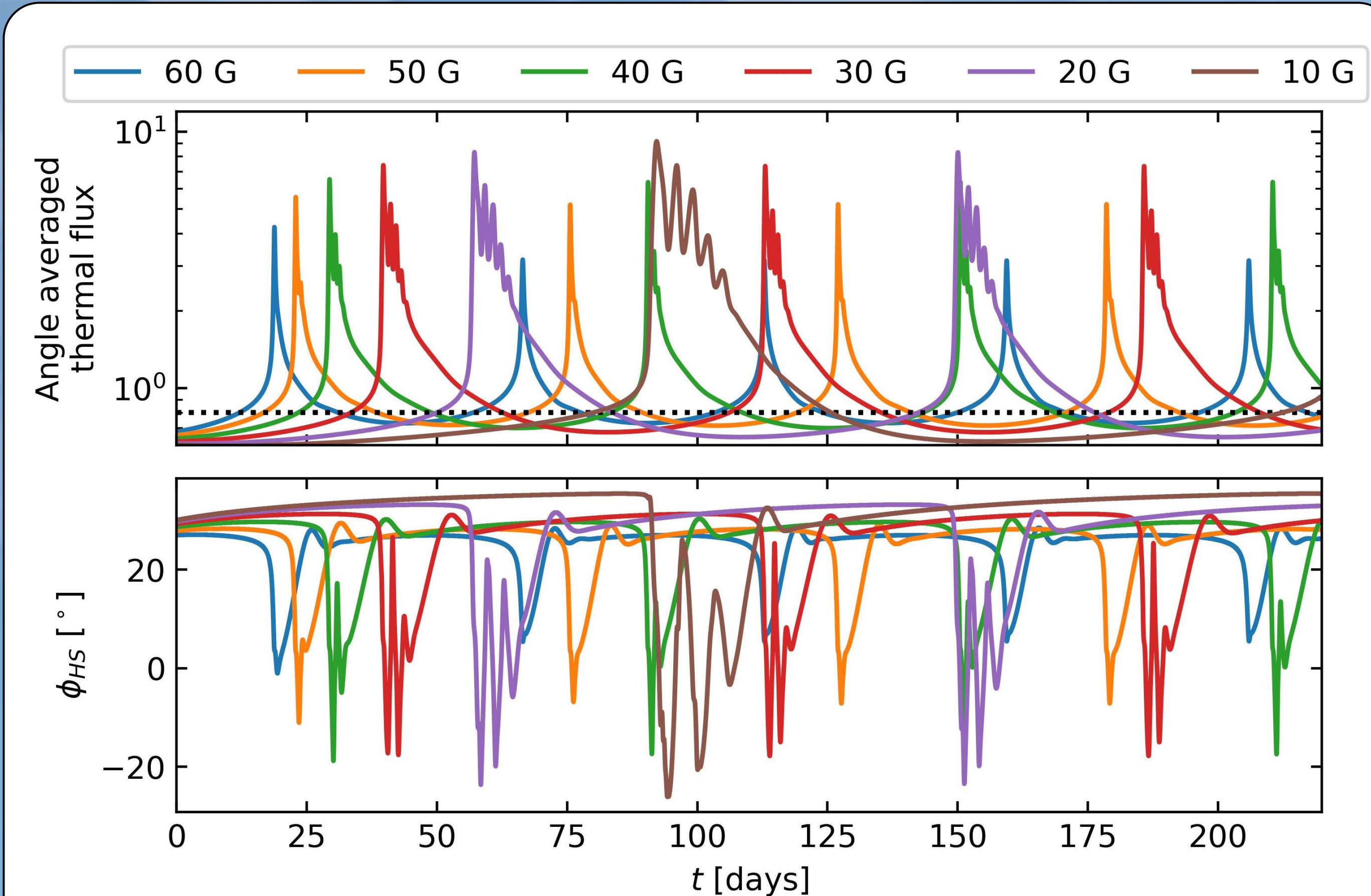


Figure 3 : Angle averaged thermal flux on the dayside of the planet for different values of magnetic field, and the offset of the peak of the thermal flux; the hot spot.

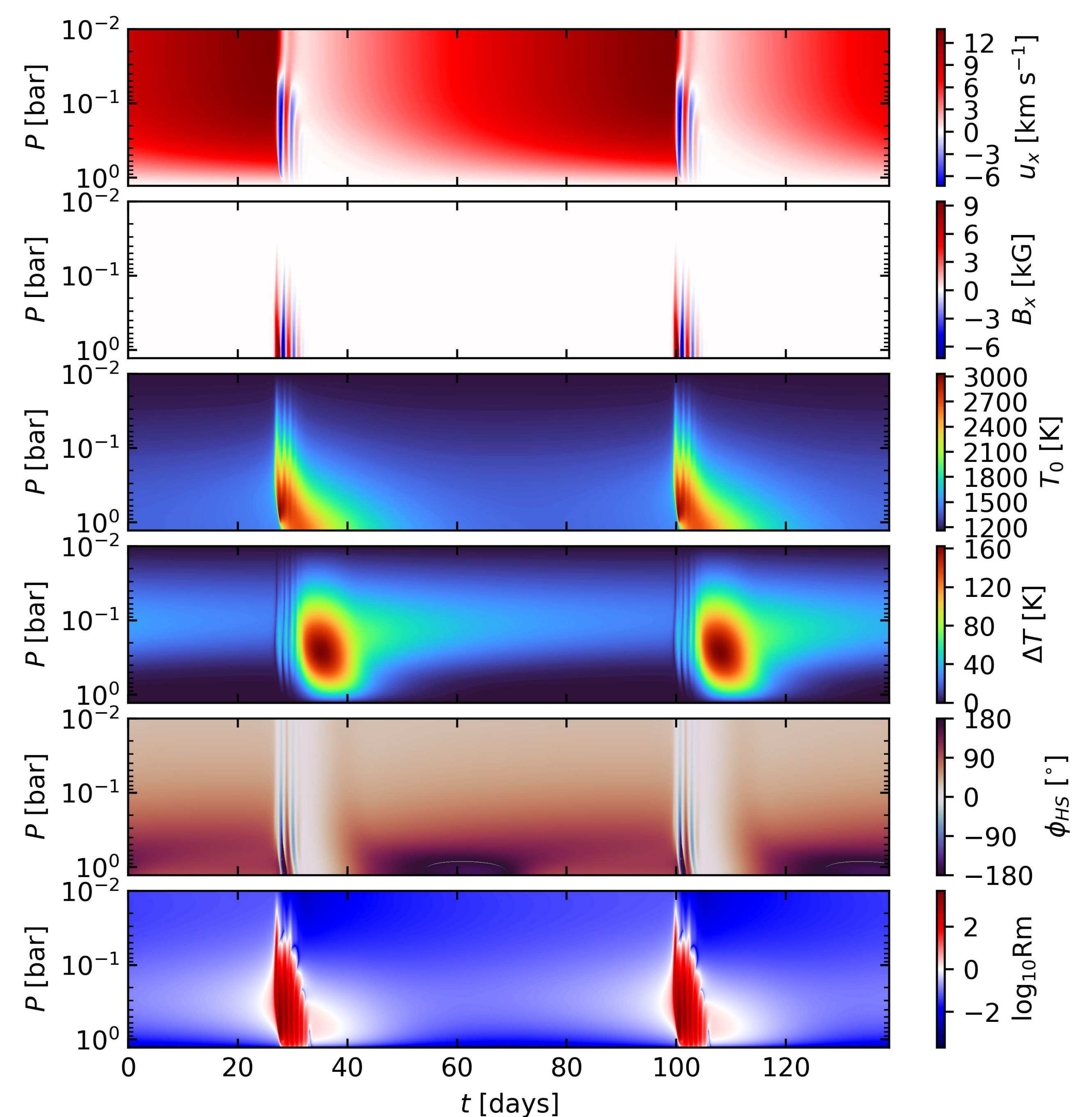


Figure 2 : From top to bottom : Spatiotemporal evolution of the velocity, magnetic field, mean temperature, and peak-to-peak temperature at every layers, hot spot offset and magnetic Reynolds number in P - t . The system evolution in this figure is focused on the Alfvénic oscillations and the following cooling cause by TRI.

5. CHAOTIC TEASER

We applied the longitudinal expansion to the dimensionless local model of Hardy et al. 2022. While general motions are the same, **chaotic behavior was found!** (Figures 4 and 5)

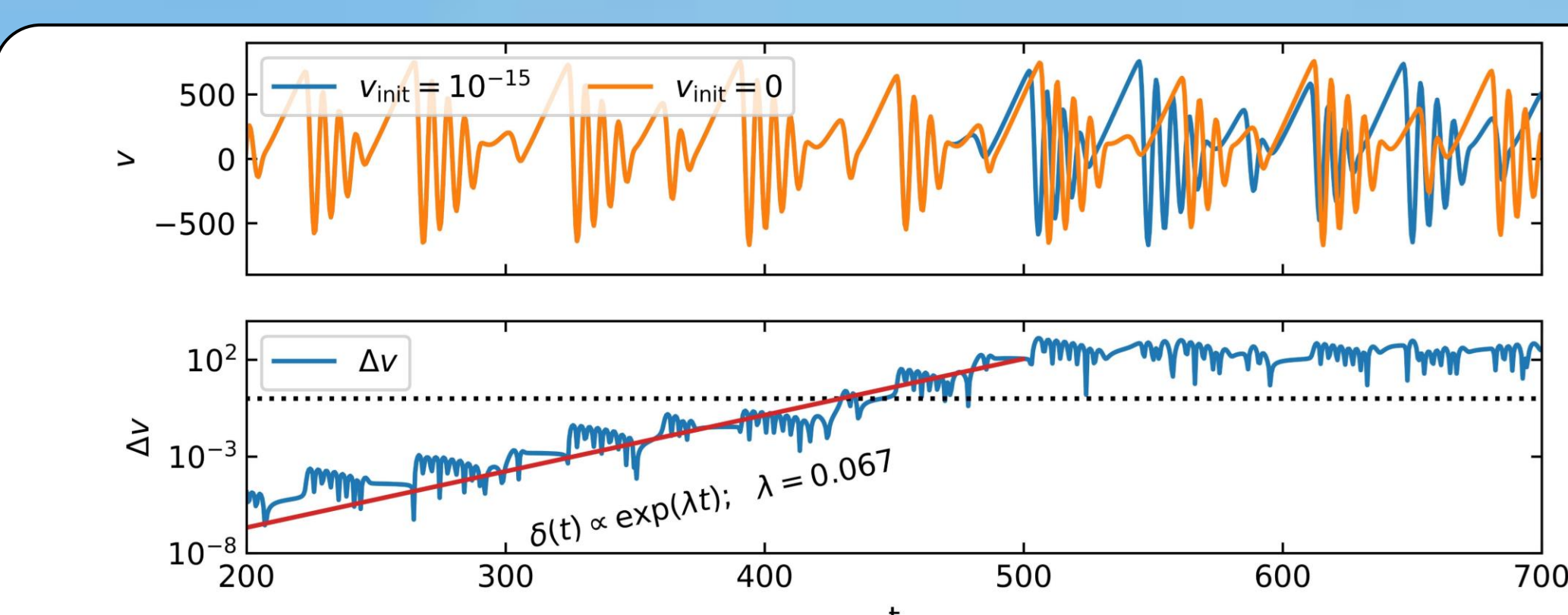


Figure 4 : Decorrelation between unperturbed and perturbed solutions with the associated Lyapunov exponent.

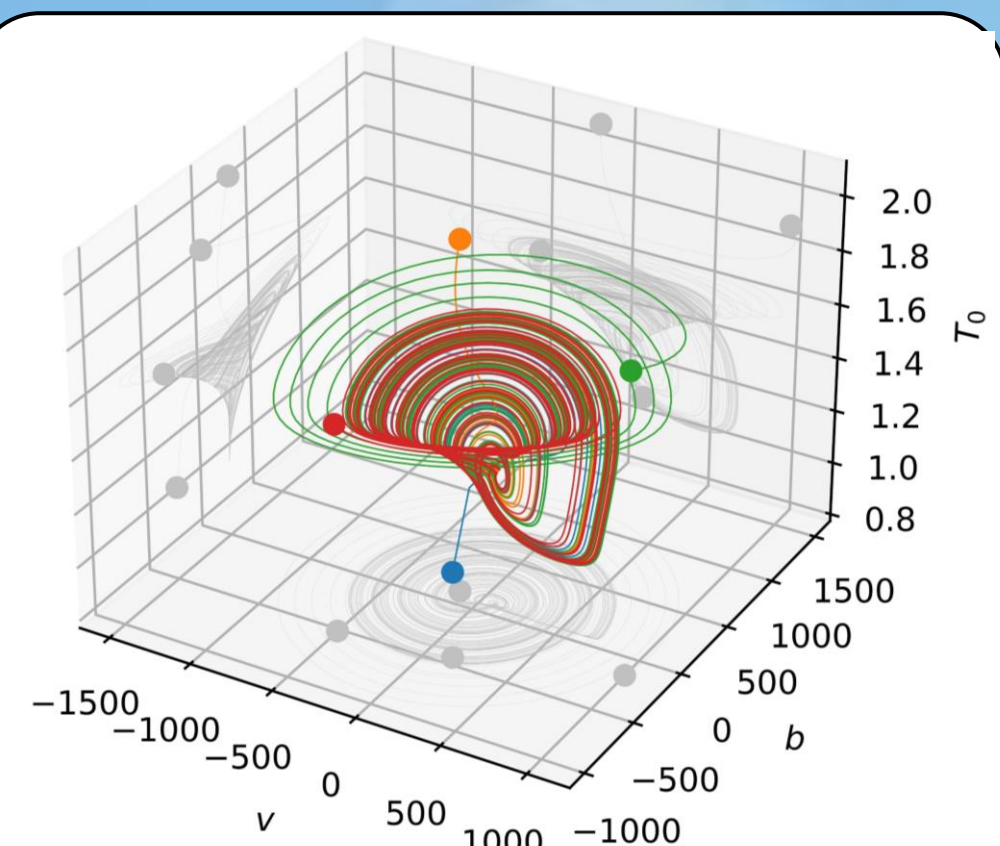


Figure 5 : 3D phase space of chaotic solution with different initial conditions, converging onto the strange attractor.

raphael.hardy@umontreal.ca

REFERENCES

- Bell, T. J., Dang, L., Cowan, N. B., et al. 2021, MNRAS, 504, 3316, doi: 10.1093/mnras/stab1027
 Hardy, R., Charbonneau, P., & Cumming, A. 2023, ApJ, 959, 41, doi: 10.3847/1538-4357/ad0968
 Hardy, R., Cumming, A., & Charbonneau, P. 2022, ApJ, 940, 123, doi: 10.3847/1538-4357/ac9bfc
 Keating, D., Cowan, N. B., & Dang, L. 2019, Nature Astronomy, 3, 1092, doi: 10.1038/s41550-019-0859-z
 Menou, K. 2012, ApJL, 754, L9, doi: 10.1088/2041-8205/754/1/L9
 Rogers, T. M., & Komacek, T. D. 2014, ApJ, 794, 132, doi: 10.1088/0004-637X/794/2/132
 Yadav, R. K., & Thorngren, D. P. 2017, ApJL, 849, L12, doi: 10.3847/2041-8213/aa93fd